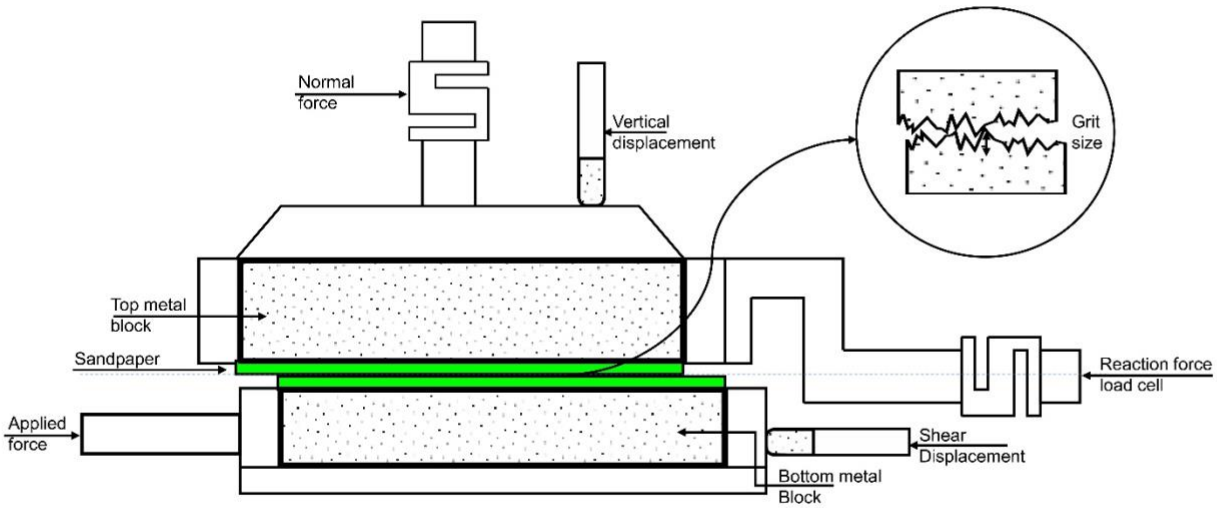

Effect of Cyclic Shearing on Contact Surfaces of Geo-Materials under Constant Normal Force

Author 1

- Pedro Ferreira, Senior Lecturer
- University College London, Gower Street, London, WC1E 6BT, UK
- E-mail: p.ferreira@ucl.ac.uk, ORCID number: 0000-0002-4626-7443

Author 2

- Tanner Muturi, MSc Student, PHD candidate
- Civil Engineering Program, Middle East Technical University, Northern Cyprus Campus, Kalkanli, Guzelyurt, North Cyprus, via Mersin 10, Turkey
- Email: tanner.muturi@metu.edu.tr

Author 3

- Abdullah Ekinci, Assistant Professor
- Civil Engineering Program, Middle East Technical University, Northern Cyprus Campus, Kalkanli, Guzelyurt, North Cyprus, via Mersin 10, Turkey
- Email: ekincia@metu.edu.tr, ORCID number: 0000-0002-6787-9983 (corresponding author)

Abstract

A large amount of research has been done on conforming surfaces in rock joints as well as on the contact between individual grains, however, not much exist in nonconforming contact surfaces subjected to friction, such as flat contacts between ballast particles, stone columns or riprap; applications that involve the use of coarse gravel subjected to low vertical stresses. Therefore, this article aims to study changes in contact properties between non- conforming flat contacts between large geomaterial particles that have been subjected to cyclic shearing under a constant low vertical force, using a direct shear apparatus. Two different silica carbide sandpapers that do not loose particles were used, to simulate different morphologies, a nominally fine and a coarse surface texture. The results show a passivation of the shear strength where a constant value of friction coefficient is reached after around 15 to 17 cycles for all tests, except the tests at the lowest vertical force. For the tests at the highest vertical force similar friction coefficients were determined for the coarse and fine surfaces. The mass broken during the 10th and 20th cycles was collected at the end of the tests and seem to show a linear relationship with the vertical force used in the test. Particle analysis, determined via microscopy, show that the grading is dependent on the initial topography of the surfaces. Despite being subjected to 10 and 20 cycles of shearing, the broken particles look similar in shape with sharp, jagged edges and having different shapes and roundness values with a large variation, indicating that the breakage was not enough to fill in the space between the particles.

Keywords:

particle-scale behaviour; repeated loading; microscopy; shear; nonconforming

List of notations

μ_c	is the friction coefficient
F_h	is the shear force
N	is the normal force
ML	is the mass loss
PSD	is the particle size distribution

1 Introduction

Cyclic shearing in the contacts between particles of geo-materials (aggregates, ballast, stone columns, rocks, etc.) are applied either naturally through earthquakes, thermal cycles, wave loading, etc, or are a consequence of its intended use, for example through railway motion or construction processes. Cyclic shear loadings will lead to wearing and the passivation of the contact surfaces of granular materials or rock interfaces. This deterioration of the shear strength is related to changes in the mechanical parameters of the geo-material strata and has been the subject of many research articles.

The effect of asperity morphology (Zhang et al. 2019), influence of boundary conditions such as monotonic shearing under constant normal loading (Barton 1973; Jiang et al. 2020), led to the development of many equations to describe the shear strength of rock joints under monotonic shearing and constant normal load as a function of the asperities shape. Similar approaches were also adopted by Indraratna et al. (1999) on surfaces with different fillings and Liu et al.(2019) on the shear of multi-joint specimens.

Cyclic shearing under a constant normal loading was investigated by Jaeger (1971) and Plesha (1987). Their results showed that specimens have a high shear stress in the first cycle, with obvious peaks and residual shear stresses until the number of cycles (N) is larger than 15. Han et al. (2020) carried out a similar study on unfilled and infilled rock joints under constant normal stiffness, concluding that the shear stress (t), normal stress (σ_n) and vertical displacement (δv) for both cases decrease with the increase in the number of cycles. This phenomenon is caused by the shearing of asperities in the initial cycles with subsequent cycles subjected to lower friction. Sliding behavior is also likely to occur on asperities with low amplitude, under low normal stresses, as observed by Zhang et al. (2019). Xiao et al. (2020) stated that crushing leads to a change in grading resulting in a decrease in strength and dilatancy as well as an increase in compressibility, with the amount of grain crushing, experienced during shearing, influenced by the stress level, coordination number, shape, grain size, specimen size and stress path. Niktabar et al. (2017) showed that shear strength is seen to be higher when the asperity angle was higher, however, higher angles experienced faster decreases in shearing strength in subsequent cycles. Utilizing experimental results from previous studies Wang and Tonon (2009) created a 3D DEM model using spherical particles. Furthermore, Kazerani and Zhao (2010) stated that the main problem is the definition of micro-parameters for DEM codes using bonded particle modeling to simulate breakage. More recently, polygonal rigid particles were used by Maciejewski et al. (2020) to model the interface of rock joints under cyclic loading where good results were obtained.

In recent years, researchers developed custom-built apparatus to explore the mechanics of grain contact behavior of a broad range of geo-materials, achieving significant development on the contact response of single grains (Cole and Peters 2007; Cole et al. 2010; Cavarretta et al. 2011; Senetakis and Coop 2014; Yang et al. 2016; Cole and Hopkins 2017; Nardelli et al. 2017). Results from experimental research have shown significant influence from the material type and the morphological characteristics of the contacts, similar to the response of granular materials are rock interfaces (Cavarretta et al. 2010; Hanaor et al. 2013; Sandeep and Senetakis 2018; Sandeep et al. 2018, Sandeep et al. 2021). These experimental tests have helped the development of numerical models and contact relationships that better explain the shear behavior of contact points in geo-materials.

Furthermore, there have been a lot of work on friction between nonconforming surfaces in the geophysics research community (focusing on the dynamics of earthquake fault gouges) in the context of rate-and-state friction laws. Those studies looked at many frictional scenarios between nonconforming rock surfaces, including cyclic loading. The generation of fines have also been studied where authors looked at the grain size distribution produced from shear surfaces (Marone 1998; Collettini et al. 2009; Im et al. 2020; Trugman et al. 2020; Zoet et al. 2020).

This study is an initial attempt to understand the shearing properties of non-matching or non-conforming surfaces, equivalent to the behavior of flat multi mineral contacts that occur in large granular materials used for ballast, stone columns and riprap, during cyclic or thermal loads, normally subjected to low vertical forces. Something very difficult to find in the literature. Therefore, this paper shows results of cyclic shearing under low and constant normal force conditions. This was obtained by using a conventional direct shearing equipment and artificially manufactured samples. The broken particles are also analyzed, using images from a microscope and a free to download software. This work makes a significant contribution to understand factors effecting variations in friction coefficient such as vertical forces, particle breakage, morphology and minerology. Results will lead to development of an assessment method that will allow representation of geo-material surface behavior to calibrate current DEM models and notably affect the accuracy of the DEM analysis.

2 Methodology

2.1 Sample preparation

Metal disks manufactured to a tight fit in a 64mm diameter shear box had Coarse sandpaper #40 (0.425mm grain size) and fine sandpaper #80 (0.201mm grain size) glued to one of the flat surfaces. The sandpaper used in the experiment is for use in wet sanding of metals and it was selected because it is almost impossible to remove particles from the sandpaper. Different grades of sandpaper were used to represent different surface morphologies that could be identified by a single number that represent the coarseness of the mineral particles. Once the sandpaper was glued to the metal blocks, these were fixed into the shear box, preventing displacement and rotation during shearing.

2.2 Direct shear testing

A conventional semi-automatic direct shear apparatus was used to shear the samples. Figure 1 shows the schematic diagram of the shear box setup. Tests were carried out using normal forces of 200 N, 400 N and 600 N, for 10 and 20 cycles on both surfaces, from now on designated coarse and fine.

A 1mm/min shearing rate was used until 3mm of displacement were achieved and the direction of shearing was reversed until the initial starting point was reached. The shear displacement and the shear force were only recorded during the forward motion of each cycle. After 10 or 20 cycles, the test was finished and the shear box was carefully disassembled, and the broken particles were collected and weighed.

It was reported by Jaeger (1971) and Plesha (1987) that specimens have a high shear stress in the first cycle, with obvious peaks and residual shear stresses until the number of cycles (N) is larger than 15. Therefore, it was decided to finish the tests at 10 and 20 cycles. Where 10 cycles were considered enough in the stability zone to generate a good breakage and 20 cycles was considered enough to have achieved a constant friction.

2.3 Microscopy

To investigate changes in the surface morphology, microscopic images using an Olympus™ SZX16 Stereo Microscope were taken from all samples tested under 600 N of normal force. Images were obtained from 5 different points on the surface of the bottom sandpaper at a magnification of 3.2X. The images were taken before shearing and, after shearing, before and after removal of the broken particles. Under the microscope, the longest dimension of 100 randomly selected broken off particles, from both samples, were measured along their longest length (similar to the Feret's diameter), given the limitation of the software version used. ImageJ software was later used to analyse and determine the particle size distribution of the broken particles using the same images

3 Results and Discussion

3.1 Effect of Cyclic Shearing

Figures 2 compares the variation of horizontal shearing force versus horizontal displacement for all samples tested to 20 cycles. The colours represent groups of 5 cycles with the first 5 cycles plotted in blue, the second set of 5 cycles plotted in brown, followed by followed by grey and yellows to represent the third and fourth set of cycles. All tests show an increase in the shearing force with an increase in normal force, consistent with results by Jiang et al. (2020) and others. With the colour system is easy to see that with the increase of number of cycles, a stabilization and a reduction in the shear force was observed. Also, a closer observation of the initial linear portion of the graphs, show that the shear stiffness is seen to be linear and proportional to the applied normal load. Despite the difficulty in determining the starting point in some of the loading stages, this observation aligns with those made by Kulatilake et al. (2016), in which joint shear stiffness was found to be a linear function of the applied normal stress. Furthermore, the first 5 cycles applied to the coarse sample show a large variation in shear force for the vertical force of 200N, not seen in the fine sample. This large variation is likely to be caused by the breaking of the asperities in the initial cycles as observed by Han et al. (2020). Under the 200 N force, a frictional sliding was observed for the fine sample, with very low breakage. This is consistent with observations made by Zhang et al. (2019). With an increase in the number of cycles, breakage starts reducing and less variations are observed in the curves, similar to the observations made by Han et al. (2020).

The friction coefficient was calculated as $\mu_c = F_h/N$, where N is the normal force and F_h is the shear force and Figure 3a shows the average shear force and the friction coefficient response after 1mm displacement on each cycle, for all tests. The shear force is reducing with the increase in number of cycles and this reduction is steeper for the higher normal force. This arises as asperities are being crushed, leading to a change in the morphology of the contact surface; broken particles fill the voids, rotate and create more contact points, reducing the resistance to shearing, as seen also in the literature. These observations are consistent with those of Niktabar et al. (2017).

Figure 3b also shows that in the first cycle, the initial friction coefficient seems to be dependent on the asperities; being much higher for the coarse than the finer samples. The difference between the friction coefficients of the coarse and fine samples, at 200N, seem to be constant after 15 cycles, despite the scatter in the data. These findings confirm those of earlier studies, such as Jaeger (1971) and Plesha (1987). As the vertical force increases this difference reduces and, at 600N, the friction coefficient for fine and coarse samples is similar and approximately equal to 0.58. This result is similar to the results obtained by Bian and Wu (2015), for a clutch friction test on Silica Carbide (SiC), the same material used in the manufacture of this sandpaper. Their results show a variation from approximately 1 to around 0.58 to 0.62 after a large number of cycles. This shows that the dependence of the friction coefficient in the surface morphology reduces as the vertical force increases, becoming dominated by the vertical force after a threshold is reached. If the vertical force is high enough the minimum friction coefficient of the material can be reached at a lower number of cycles. Table 1 shows the average rate of variation of the friction coefficient with the number of cycles. It is clear, however clear in the picture that the friction coefficient has a much larger variation between the few initial cycles, therefore the average variation may not be a good parameter to determine how the friction coefficient changes with the number of cycles and can only be used between cycles 15 and 17 as afterwards changes seen are very small for all tests. Nevertheless, the table shows a linear correlation between the average value and the number of cycles.

The difference in shear force (ΔF_h) and friction coefficient ($\Delta \mu_c$) with regards to the first cycle, were plotted in Figure 4, against the normal force on cycles 10 and 20. It is clear that by increasing the normal force there is an increase in ΔF_h and $\Delta \mu_c$ with the coarse surface showing larger differences in all parameters. The linear regressions presented in Figure 4 are just to show that the data seems to be linear with the slope of the line not showing a variation as large as the intercept, since the number of cycles will control the location of the line.

Figure 5 shows the measured mass loss (ML) plotted against the normal force for cycles 10 and 20. ML is a measurement of breakage on the surface and the figure shows that increasing the vertical force creates more breakage with the coarser surface showing the largest breakage values. The relationship between ML and vertical force seems to be linear, however a dashed line was plotted from 200N to zero, to indicate that the breakage is not linear at lower forces and tests at lower stresses would be needed to determine it. Although there are no values of ML for every cycle, it is clear that every cycle would have a line parallel to the ones plotted in the graph and, at a large enough number of cycles, breakage should cease. Similar trends have been reported by Ferreira and Coop (2020) in their work on factors effecting terminal grading of sands. From figures 4 and 5, the data from the 10th cycle was plotted against the data from the 20th cycle in Figure 6, since there seems to be a linear correlation between the reduction of shear force and friction coefficient and an increase in mass loss reduction between these cycles. The results show that despite the initial starting point, the changes from 10th cycle plotted against the 20th seem to align on a straight line passing through the origin, indicating a unique relationship between any number of cycles.

The initial group of points represents the fine surface whilst the points located further to the origin represent the coarse surface. Within their groups, the points are organized by vertical force with the highest force being the furthest away from the origin. Knowing the relationship between the number of cycles would allow the prediction of the mobilized quantities at higher number of cycles, without the need to test the samples. To improve this relationships, plots of different number of cycles can be prepared in order to understand how the slope of these lines change and if it is possible to determine a limit on this variation, indicating that these parameters achieved a critical value.

Therefore, this will enable the determination of the current condition of the granular material with simple measurements and the prediction of how long it will take until the resistance reaches a critical value or maintenance is required. Furthermore, these relationships can be useful to obtain parameters via simple tests for numerical analysis of the current and future conditions of the granular material.

3.2 Microscopic Observations

To understand the breakage caused by the shearing, the surfaces before and after 10 and 20 cycles were analysed under a microscope. Figure 7 show the microscopy images using a 3.2x magnification and 600N vertical force: on the left images of the sand paper before shearing; in the middle, images of the shearing area with the broken particles for 10 and 20 cycles and, on the right, images of the same area after collecting the broken particles. For the coarse samples the broken particles after 10 cycles seem to have had the asperities chipped of from the edges of larger particles whereas after 20 cycles the damage to the particles seem to have increased, although it is difficult to detect. This observation can be correlated to Figure 5, where the ML difference between 10 and 20 cycles is not very large. For the fine sample, it is difficult to see large changes; the pictures with broken particles clearly show a larger number of broken particles for cycle 20 and this is confirmed by Figure 5. However, once these are removed, the differences are subtle, as they are more concentrated at the tips of the protruding grains.

The results of the measurements of the longest dimension of 100 randomly selected particles was plotted as a particle size distribution (PSD) in Figure 8. The dimensions of the particles from the coarse samples have the widest variation in size with the smallest being around 0.026mm and the largest being around 0.364mm, with an average size equal to 0.1423mm. For the fine sample, the smallest particle measured was 0.035mm and the largest particle 0.199mm, with an average size of 0.089mmm. The same images were later analysed using ImageJ, an open-source software for image analyses that can detect edges and perform calculation of certain particle descriptors. ImageJ was used to determine the area of the particles in the images allowing the calculation of the diameter of a circle with similar area (equivalent diameter – ED). The data was converted in PSDs and plotted also in Figure 8. As expected, the ED has a distribution showing smaller sizes; the largest for the fine sample is 0.126mm and the coarse 0.233mm, compared to the previous curves. Given the high resolution of the images and the nature of the software, the number of smaller particles detected was quite large. These were included in the calculations of % passing for both curves, however the plots were truncated at 0.01mm in size. As can be seen the PSDs are quite similar in shape and seem to indicate that the PSDs of the broken particles are dependent on the initial morphology of the contact surface.

Figure 9 shows a picture of the particles analysed under the microscope and the roundness $[4 * Area/(\pi * Major\ axis^2)]$ plotted against particle size (ASTM D7971-20). The picture depicts the shape of the grains; angular with jagged sharp edges, characteristic of broken particles. Although they have been subjected to shear cycles, the results from roundness show that there is a wide variation of values in all sizes of particles and these are not dependent on the type of surface being tested.

These results are important as when flat contacts are established between large aggregates the loading cycles will create a granular film between the surfaces that will reduce the friction coefficient. If the loading cycles continue, they generate an infill of granular material that should stop breakage and allow the contact to arrive at a constant friction coefficient.

4 Conclusions and Recommendations

- The results show that with the increase in the number of cycles there is a reduction in the shear force with a consequent reduction in the friction coefficient.
- The reduction of the friction coefficient seems to be governed by the surface morphology for lower normal forces. As the normal force increases, the importance of the morphology reduces and a similar friction

coefficient between coarse and fine shear surfaces can be determined, indicating that after a force threshold exists.

- The change in shear force between the 10th and 20th cycle is only 37% higher than between the beginning of the test and the 10th cycle for all samples. Similarly, the mass broken between cycle 10 and 20 is only 28% bigger than the mass broken in the first 10 cycles.
- The particle size distribution of the broken particles is dependent on the surface morphology with rougher surfaces generating wider particle size distributions, this difference was seen in both, manual measurements and image analysis using ImageJ.
- It is recommended that various surface textures, increased number of cycles and normal forces are applied so a "threshold" beyond which no further changes observed can be determined. It is also recommended to test materials which have different mineralogies.

Declarations

Funding

The authors express their appreciation to Office of Research Coordination and Support, Middle East Technical University, Northern Cyprus Campus for funding this research group. Scientific Research Project Code FEN-20-YG-4.

Conflicts of interest

The authors have no conflicts of interest to declare that are relevant to the content of this article.

Availability of data and materials

The datasets generated during and/or analysed during the current study are available from the corresponding author on request.

References

ASTM-D7971-20 (2020) Standard Guide for Measuring Roundness of Glass Spheres Using a Flowing Stream Digital Image Analyzer. West Conshohocken, PA; ASTM Int

Barton N (1973) Review of a new shear-strength criterion for rock joints. Eng Geol 7:287–332

Bian G, Wu H (2015) Friction and surface fracture of a silicon carbide ceramic brake disc tested against a steel pad. J Eur Ceram Soc 36:3797–3807

Cavarretta I, Coop M, O'Sullivan C (2010) The influence of particle characteristics on the behaviour of coarse grained soils. Geotechnique. https://doi.org/10.1680/geot.2010.60.6.413

Cavarretta I, Rocchi I, Coop MR (2011) A new interparticle friction apparatus for granular materials. Can Geotech J 48:1829–1840

Cole DM, Hopkins MA (2017) The contact properties of naturally occurring geologic materials: contact law development. Granul Matter 19:1–17

Cole DM, Mathisen LU, Hopkins MA, Knapp BR (2010) Normal and sliding contact experiments on gneiss. Granul Matter 12:69–86

Cole DM, Peters JF (2007) A physically based approach to granular media mechanics: grain-scale experiments, initial results and implications to numerical modeling. Granul Matter 9:309–321

Collettini C, Niemeijer A, Viti C, Marone C (2009) Fault zone fabric and fault weakness. Nature 462:907–910

Ferreira PMV, Coop MR (2020) Factors that influence the terminal grading of sands. Géotechnique Letters 10:4, 518-523.

Han G, Jing H, Jiang Y, et al (2020) Effect of cyclic loading on the shear behaviours of both unfilled and infilled rough rock joints under constant normal stiffness conditions. Rock Mech Rock Eng 53:31–57

Hanaor DA, Gan Y, Einav I (2013) Effects of surface structure deformation on static friction at fractal interfaces. Géotechnique Letters 3:2, 52-58.

Im K, Saffer D, Marone C, Avouac JP (2020) Slip-rate-dependent friction as a universal mechanism for slow slip events. Nat Geosci 13:705–710

Indraratna B, Haque A, Aziz N (1999) Indraratna, B., A. Haque, and N. Aziz. "Shear behaviour of idealized infilled joints under constant normal stiffness. Geotechnique 49:331–355

Jaeger JC (1971) Friction of rocks and stability of rock slopes. Geotechnique 21:97–134

Jiang Q, Yang B, Yan F, et al (2020) New Method for Characterizing the Shear Damage of Natural Rock Joint Based on 3D Engraving and 3D Scanning. Int J Geomech 20:06019022. https://doi.org/10.1061/(asce)gm.1943-5622.0001575

Kazerani T, Zhao J (2010) Micromechanical parameters in bonded particle method for modelling of brittle material failure. Int J Numer Anal methods Geomech 34:1877–1895

Kulatilake PH, Shreedharan S, Sherizadeh T, et al (2016) Laboratory estimation of rock joint stiffness and frictional parameters. Geotech Geol Eng 34:1723–1735

Liu R, Han G, Jiang Y, et al (2019) Shear behaviour of multi-joint specimens: Role of surface roughness and spacing of joints. Geotech Lett 10:113–118. https://doi.org/10.1680/jgele.19.00044

Maciejewski J, Bąk S, Ciężkowski P (2020) Modelling of rock joints interface under cyclic loading. Stud Geotech Mech 42:

Marone C (1998) Laboratory-derived friction laws and their application to seismic faulting. Annu Rev Earth Planet Sci 26:643–696

Nardelli V, Coop MR, Andrade JE, Paccagnella F (2017) An experimental investigation of the micromechanics of Eglin sand. Powder Technol 312:166–174

Niktabar SM, Rao KS, Shrivastava AK (2017) Effect of rock joint roughness on its cyclic shear behavior. J Rock Mech Geotech Eng 9:1071–1084

Plesha ME (1987) Constitutive models for rock discontinuities with dilatancy and surface degradation. Int J Numer Anal methods Geomech 11:345–362

Sandeep CS, He H, Senetakis K (2018) An experimental micromechanical study of sand grain contacts behavior from different geological environments. Eng Geol 246:176–186

Sandeep CS, Senetakis K (2018) Effect of Young's modulus and surface roughness on the inter-particle friction of granular materials. Materials (Basel) 11:217

Sandeep CS, Li S, Senetakis K (2021) Scale and surface morphology effects on the micromechanical contact behavior of granular materials. Tribology International 159: 106929.

Senetakis K, Coop M (2014) The development of a new micro-mechanical inter-particle loading apparatus. Geotech Test J 37:1028–1039

Trugman DT, McBrearty IW, Bolton DC, et al (2020) The Spatiotemporal Evolution of Granular Microslip Precursors to Laboratory Earthquakes. Geophys Res Lett 47:

Wang Y, Tonon F (2009) Modeling Lac du Bonnet granite using a discrete element model. Int J Rock Mech Min Sci 46:1124–1135

Xiao Y, Desai CS, Daouadji A, et al (2020) Xiao, Y., Desai, C. S., Daouadji, A., Stuedlein, A. W., Liu, H., & Abuel-Naga, H. (2020). Grain crushing in geoscience materials–Key issues on crushing response, measurement and modeling: Review and preface. Geosci Front 11:363–374

Yang L, Wang D, Guo Y, Liu S (2016) Tribological behaviors of quartz sand particles for hydraulic fracturing. Tribol Int 102:485–469

Zhang X, Jiang Q, Kulatilake PHSW, et al (2019) Influence of Asperity Morphology on Failure Characteristics and Shear Strength Properties of Rock Joints under Direct Shear Tests. Int J Geomech 19:04018196. https://doi.org/10.1061/(asce)gm.1943-5622.0001347

Zoet LK, Ikari MJ, Alley RB, et al (2020) Application of Constitutive Friction Laws to Glacier Seismicity. Geophys Res Lett 47:

Table 1 – Average variation of the friction coefficient with the normal force for fine and coarse samples.

	Normal Stress (kPa)	**Mean Rate Variation**
Coarse	200	-0.008
	400	-0.010
	600	-0.013
Fine	200	-0.002
	400	-0.005
	600	-0.008

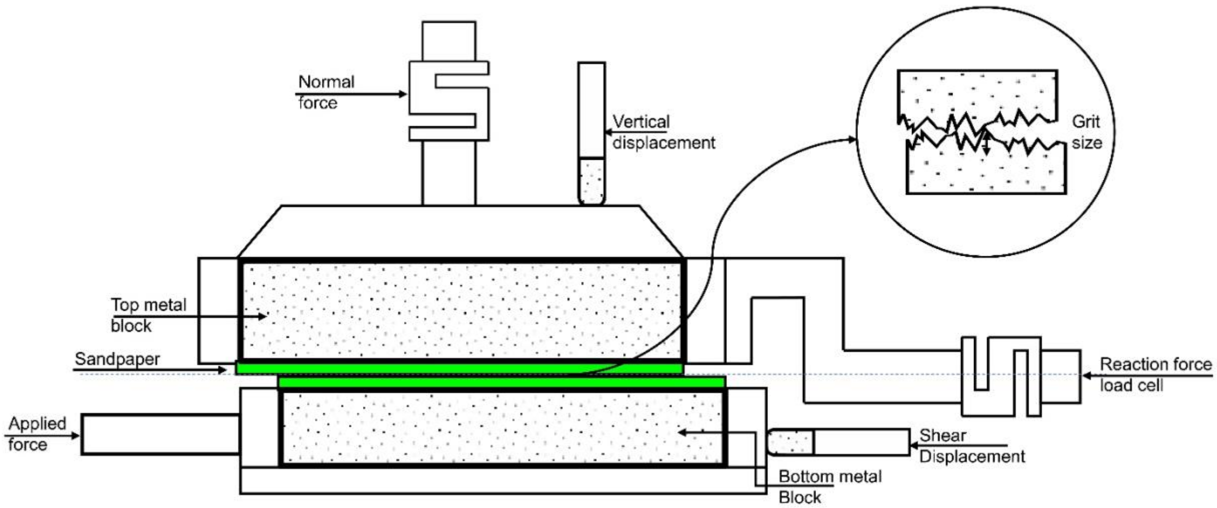

Figure 1. Direct shear cell arrangement for the specific testing condition.

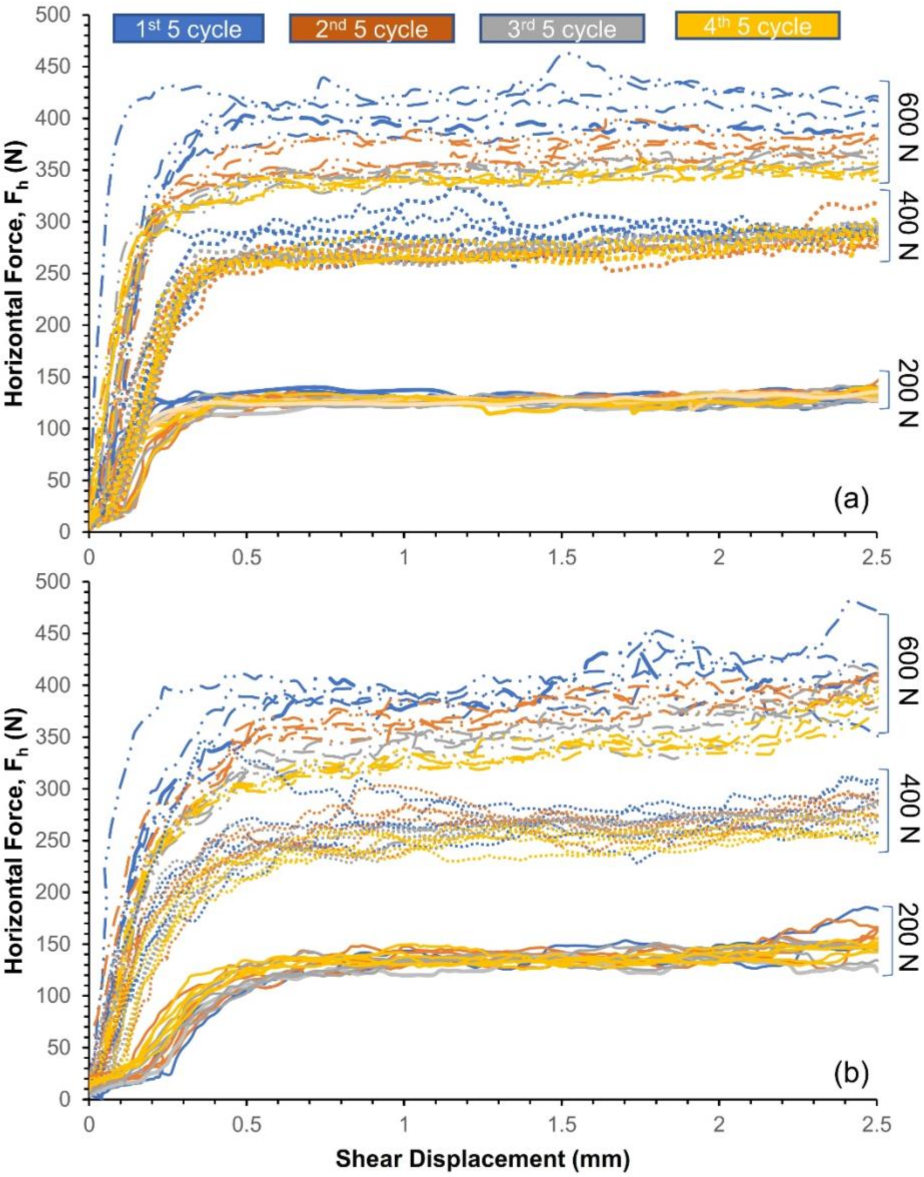

Figure 2. Horizontal force vs horizontal displacement of (a)fine and (b) coarse samples all cycles

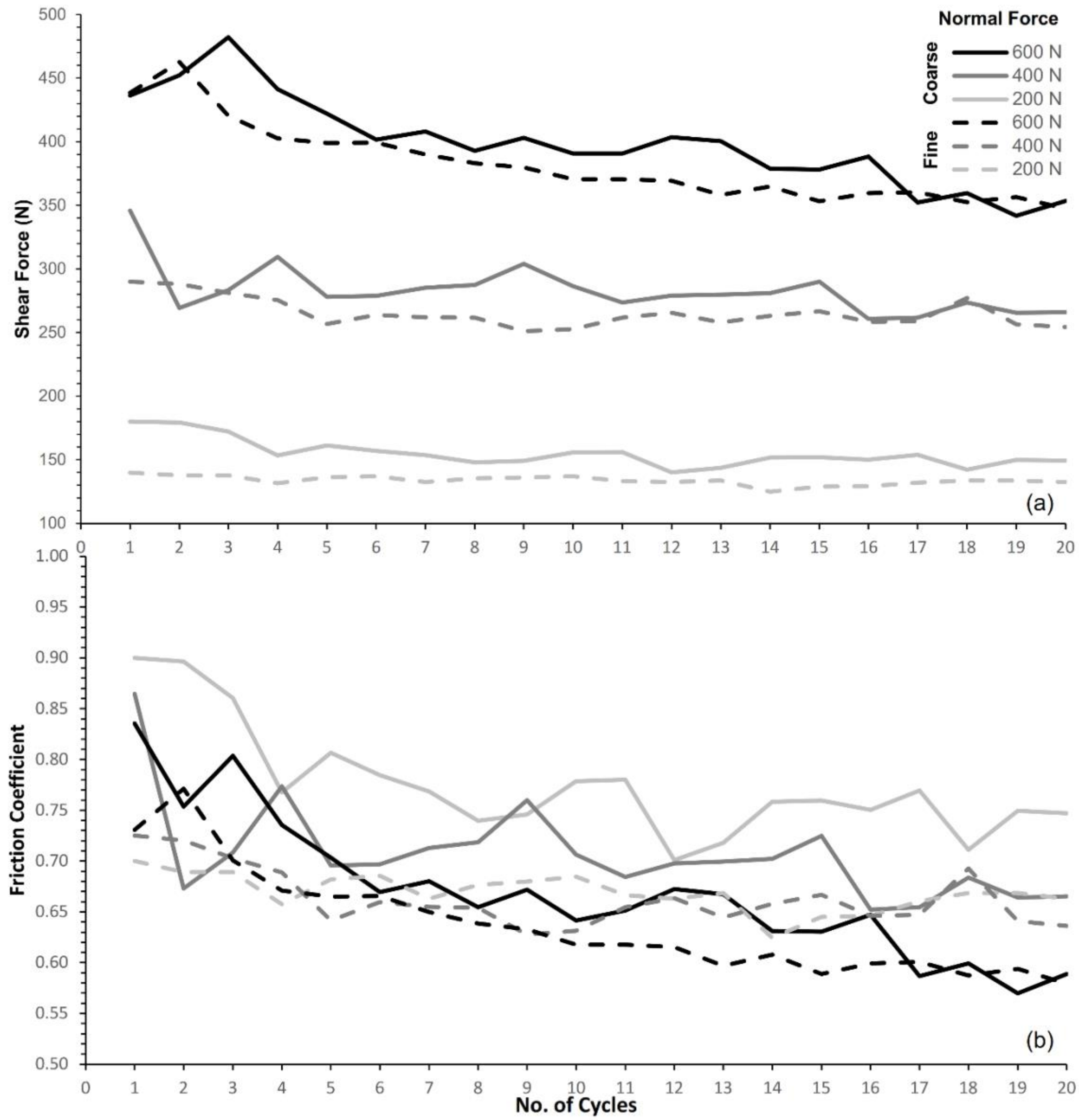

Figure 3. (a) Shear force, (b) Friction coefficient at each cycle for coarse and fine samples subjected to 600 N, 400 N and 200 N normal force.

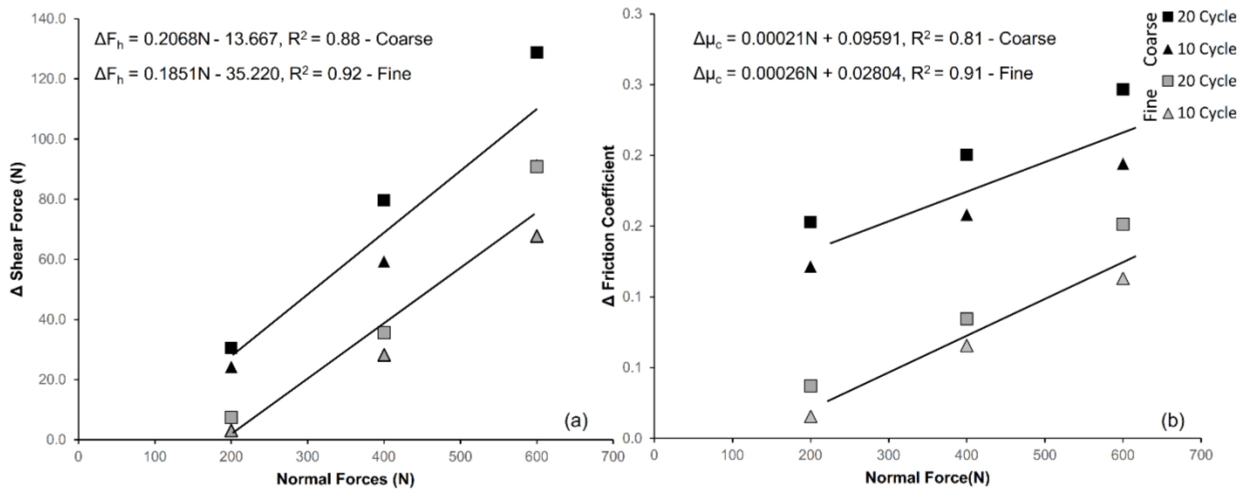

Figure 4. Reduction in (a) shear force and (b) friction coefficient vs normal force plots of fine and coarse sand at the end of 10th and 20th cycle.

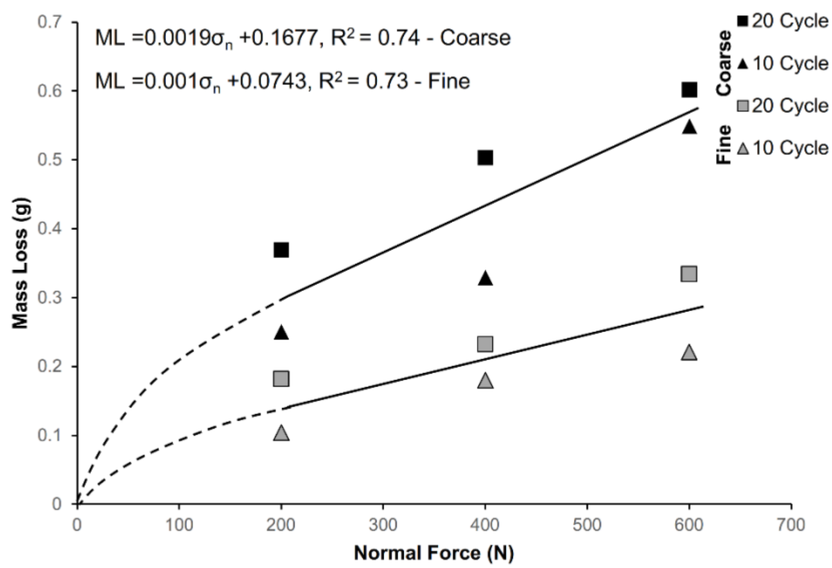

Figure 5. Reduction in mass loss vs normal force plots of fine and coarse sand at the end of 10th and 20th cycle.

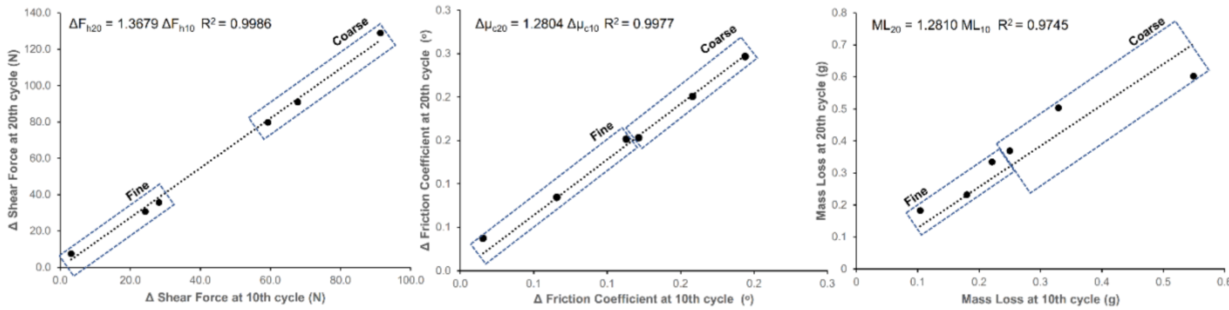

Figure 6. 10^{th} vs 20^{th} cycle relationship of a) reduction in shear force, b) reduction in friction coefficient and c) mass loss

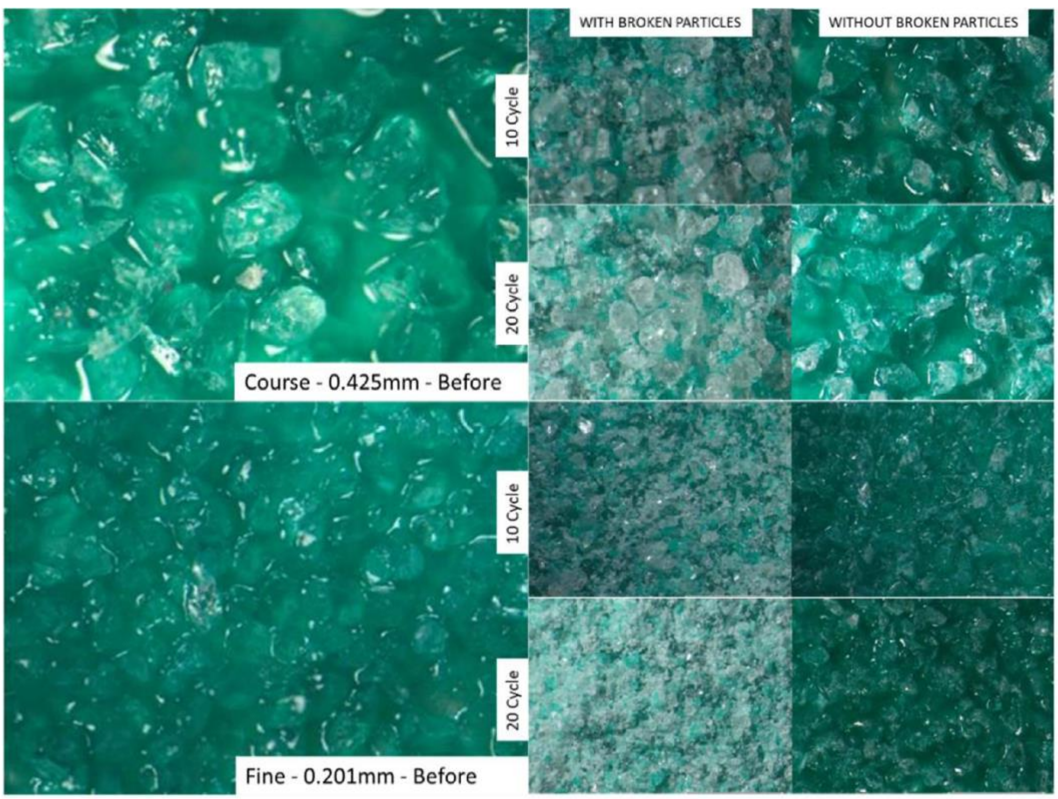

Figure 7. Microscopic image of coarse and fine samples confined to 210 kPa and 10 - 20 cycles at 3.2x magnification

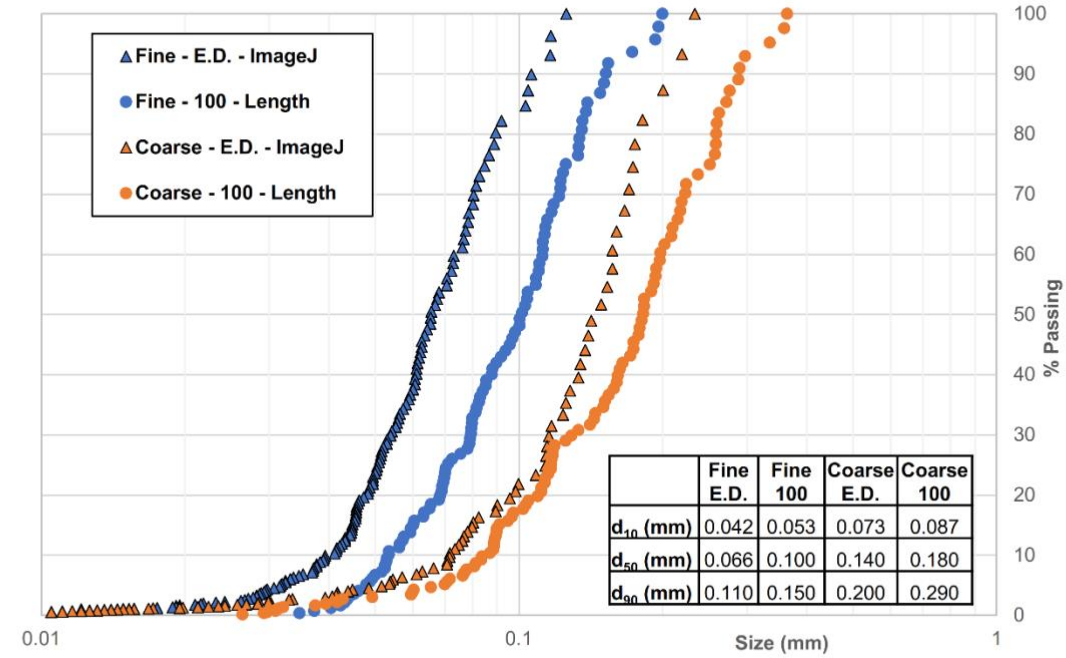

	Fine E.D.	Fine 100	Coarse E.D.	Coarse 100
d_{10} (mm)	0.042	0.053	0.073	0.087
d_{50} (mm)	0.066	0.100	0.140	0.180
d_{90} (mm)	0.110	0.150	0.200	0.290

Figure 8. Particle size distribution of 100 random particles (100-Length) and the equivalent diameter (E.D. – ImageJ) for the samples tested at 600N and 20 cycles.

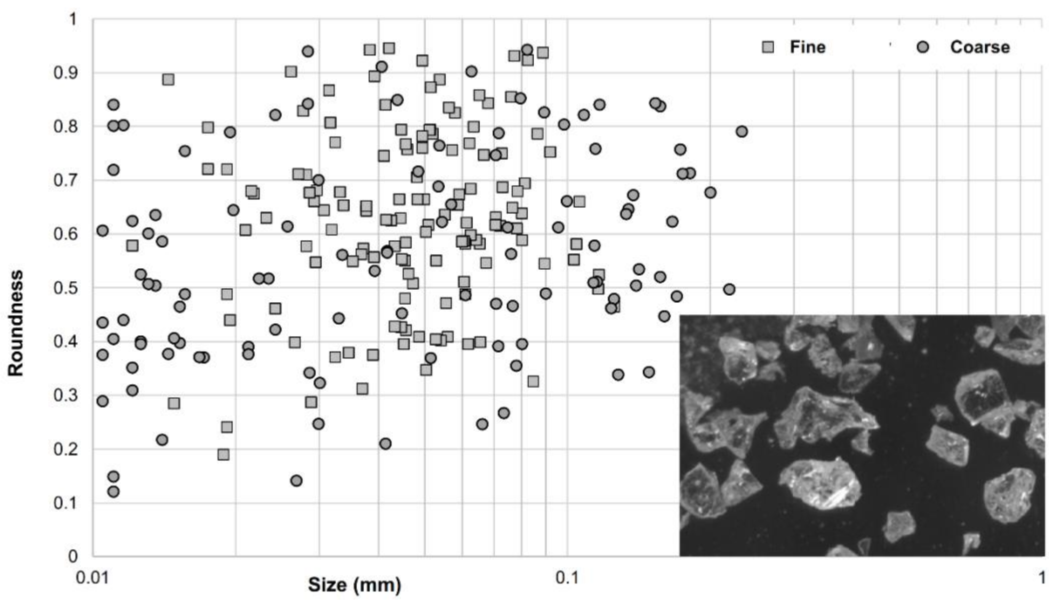

Figure 9. Particle roundness and a picture of the grains.